Ultrasonics Sonochemistry 20 (2013) 472–477

Contents lists available at SciVerse ScienceDirect

Ultrasonics Sonochemistry

journal homepage: www.elsevier.com/locate/ultson

Ultrasound-assisted copper deposition on a polymer membrane and application for methanol steam reforming

Jeong Hoon Byeon [a], Young-Woo Kim [b,*]

[a] Department of Chemistry, Purdue University, IN 47907, United States
[b] Department of Automotive Engineering, Hoseo University, Asan 336-795, Republic of Korea

ARTICLE INFO

Article history:
Received 21 December 2011
Received in revised form 29 May 2012
Accepted 5 June 2012
Available online 15 June 2012

Keywords:
Copper particles
Electroless deposition
Polymer membrane
Ultrasound
Methanol steam reforming

ABSTRACT

Copper particles were electrolessly deposited on a palladium aerosol activated polymer membrane in the presence of ultrasound. An application of ultrasound introduced a faster deposition (220 μg min^{-1} in deposition rate) and finer copper particles (9 nm in crystallite size) than those (11 and 41 μg min^{-1}; 27 and 32 nm) in the absence of ultrasound (*i.e.* respectively 20 and 45 °C in bath temperature with mechanical agitation). A better performance of methanol steam reforming (0.59 in mean conversion during 5 h operation; 1.3 and 1.6 times respectively higher than those from 20 to 45 °C cases) at a 300 °C reaction temperature was materialized for the ultrasound application, probably due to a finer (*i.e.* a more textured) copper particle deposition on a polymer membrane.

1. Introduction

The formation of metallic particles on a substrate continues to attract substantial interest because of their applications in numerous fields, such as microelectronics and optical, biomedical, space age materials, *etc.* [1,2]. Metallic particles on a porous substrate as a supported catalyst are frequently employed in a variety of reactions such as methanol synthesis, gas shift reactions, and alcohol dehydration/dehydrogenation [3]. Polymer membranes offer advantages in weight, flexibility, and elasticity relative to inorganic supports such as glasses, ceramics, and native metals [4]. Various metallic particles are usually coated on the substrate by the methods of impregnation, physical/chemical vapor deposition, sol–gel deposition, *etc.* [5]. Moreover, the performances of supported catalysts are related to the dispersity, texture, *etc.* of deposited metallic particles on substrate.

For fabricating metallic particles on a substrate with complex shapes, electroless deposition (ELD) has strong advantages over physical/chemical vapor deposition and electrodeposition, particularly with respect to its cost performance and simple equipment [6]. Normally, ELD has to be preceded by $SnCl_2$ sensitization and $PdCl_2$ activation. From the effective (blockage of active Pd sites with Sn, Cl components), economic (loss of expensive metallic components) and environmental (emission of hazardous components) points of view, as well as for simplicity in process operation, it is desirable to have an autocatalyst process without wet sensitization and activation for the deposition technology. Moreover, this technique also results in a certain number of problems, particularly at low deposition rates and uneven particle sizes [7].

The application of ultrasound during ELD generates a specific agitation due to the mechanical effect (shock wave, dispersion, *etc.*, leading to a good mixing of the chemical species) on the surface of the substrate in the bath, which leads to a faster and a finer deposition of metal [7–11] than conventional mechanical agitation.

The aim of this study is to enhance the deposition rate and dispersity of electroless Cu particles by replacing the conventional Sn–Pd wet activation with Pd aerosol nanoparticles and applying the ultrasound during Cu ELD. For comparison purposes, other ELD configurations, *i.e.* 25 and 45 °C in bath temperature with mechanical agitation, were also examined. The Cu deposited polymer membranes were then applied to methanol steam reforming as the supported catalyst. The use of the Cu deposited membrane is still limited only a few studies [3,12,13], and therefore there is not much information available concerning the appropriate fabrication process.

2. Materials and methods

The overall steps involving Pd aerosol activation were used to deposit Cu on the surface of a polymer membrane and they are schematically described in Fig. 1. The activation involves the production of Pd aerosol particles using spark discharges and their

* Corresponding author. Tel.: +82 41 540 5819; fax: +82 41 540 5818.
E-mail address: ywkim@hoseo.edu (Y.-W. Kim).

1350-4177/$ - see front matter © 2012 Elsevier B.V. All rights reserved.
http://dx.doi.org/10.1016/j.ultsonch.2012.06.002

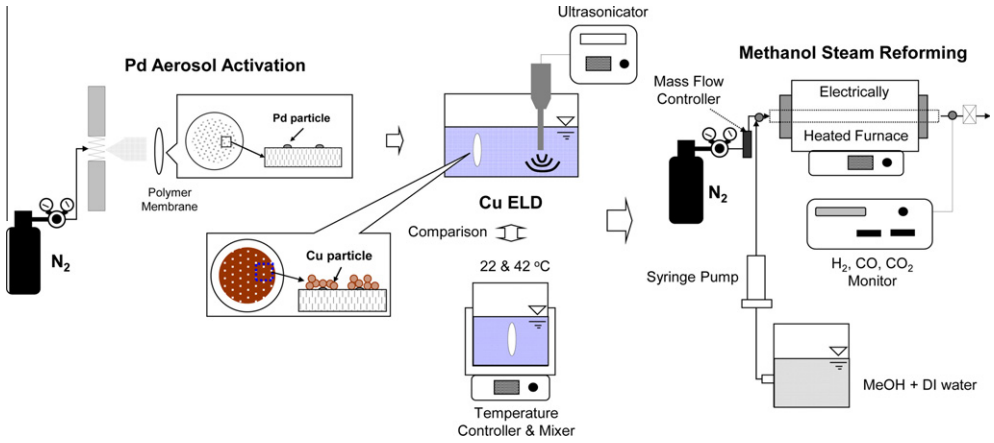

Fig. 1. Schematic of ultrasound-assisted Cu ELD on Pd aerosol activated PTFE membrane and its application for methanol steam reforming.

mechanical collection on a polymer membrane [14]. The spark discharges were a kind of atmospheric pressure nonequilibrium plasma [15]. The polymer membrane (47 mm in diameter and 0.2 μm in pore size, 11807-47-N, Sartorius) was used as a support and provided a noncatalytic surface for Cu particle deposition. A polytetrafluoroethylene was selected because of its superior chemical resistance (hydrophobicity), good thermal stability, and high mechanical strength [16]. Furthermore, the hydrophobicity of the support favored the adsorption of organic compounds over the catalyst surface [17]. The flow rate of the N_2 gas to carry the spark which produced the Pd particles was controlled by a mass flow controller (MFC, Tylan). To prevent the detachment of the Pd particles from the membrane, the membrane was separated and annealed in air at 240 °C for 10 min. Once the membrane was activated using Pd aerosol particles, the membrane was immersed in the electroless bath (100 mL) for the deposition of Cu onto the activated membrane.

Two solutions were mixed and used for the ELD bath. Solution A contained 10 g of copper sulfate, 40 g of sodium potassium tartrate (Rochelle salt), and 10 g of sodium hydroxide in 100 mL of deionized water. Solution B was an aqueous formaldehyde solution (37.2 wt.%). The two solutions A and B were mixed in a 10:1 (v/v) ratio and the activated membrane was then immersed into the mixture so that Cu particles would be coated on the Pd particles by the following reaction:

$$Cu^{2+} + 2HCHO + 4OH^- \rightarrow Cu + 2HCO_2^- + H_2 + 2H_2O \quad (1)$$

Ultrasound (VCX 750, Sonics & Materials Inc., US) at 20 kHz (frequency) and 194.8 W cm^{-2} (input power density) was applied into a bath for the Cu deposition. The ultrasound was produced parallel to the liquid surface, and the activated membrane was placed vertically. The membrane was rinsed with deionized water after it was removed from the ELD bath to remove the residual and then set aside to dry. All chemicals and membranes were used as received without any further purification.

Steam reforming of methanol was carried out in a quartz fixed bed reactor (37 mm inner diameter) at atmospheric pressure and at temperatures ranging from 180 to 300 °C. The maximum temperature was chosen as 300 °C to prevent the burn-off of the membrane [18]. The Cu deposited membrane was imbedded in the reactor, as shown in Fig. 1. Methanol was acquired from a methanol–water mixture and the flow rate of the mixture was controlled by a syringe pump. Inert gas (Ar, controlled by another MFC) was also supplied to carry the mixture into the reactor, resulting in a space time of 13,000 $m_{gas}{}^3\ h^{-1}\ m_{membrane}{}^{-3}$. To avoid the condensation of the reactant or any reaction product, all the lines were heated above 250 °C. An on-line gas chromatograph (GC-6820) was used to detect the composition of hydrogen-rich gas. The three main reactions for this combination of reactants and products can be written as the following three reactions [12,19,20]:

$$CH_3OH + H_2O \rightarrow 3H_2 + CO_2 \quad (\Delta H^o_{298} = +49.4\ kJ\ mol^{-1}) \quad (2)$$

$$CH_3OH \rightarrow CO + 2H_2 \quad (\Delta H^o_{298} = +92.0\ kJ\ mol^{-1}) \quad (3)$$

$$CO + H_2O \rightarrow CO_2 + H_2 \quad (\Delta H^o_{298} = -41.1\ kJ\ mol^{-1}) \quad (4)$$

Eq. (2) represents the methanol decomposition. Eqs. (3) and (4) represent a water gas shift reaction. The major products of the reforming process are H_2 and CO_2. A small quantity of CO is also produced. The methanol conversion X_{MeOH} and volumetric H_2 fraction y_{H_2} can be calculated by the following equations [21]:

$$X_{MeOH} = \frac{Q_e(y_{CO} + y_{CO_2})}{22.4 \times v_{MeOH}} \quad (5)$$

$$y_{H_2} = \frac{v_{H_2}}{Q_e} \quad (6)$$

where Q_e is the flow rate of effluent gas, v_{H_2} is the H_2 flow rate, y_{CO} and y_{CO_2} are the volumetric fractions of CO and CO_2, respectively, and v_{MeOH} and v_{H_2} are the molar flow rates of CH_3OH and H_2 fed into the reactor, respectively.

All experiments and measurements were performed four times and the following data are described by using the averaged values.

3. Results and discussion

Fig. 2a shows the size distribution of the spark produced Pd aerosol particles, which was obtained using a scanning mobility particle sizer (SMPS, 3936, TSI) system. The geometric mean diameter and geometric standard deviation were 29.3 nm and 1.53, respectively. The total number concentration and surface area concentration of the particles were 9.84×10^6 particles cm^{-3} and 3.74×10^{10} $nm^2\ cm^{-3}$, respectively. Fig. 2b shows the transmission electron microscope (TEM, JEM-3010, JEOL) micrograph of the Pd particles, which consisted of primary particles with a mode diameter of approximately 3 nm. Fig. 2b also shows the electron diffraction pattern corresponding to the TEM micrograph. The pattern had diffraction lines showing (111) and (200) reflections and a weak diffraction line showing (220) of the face-centered cubic lattice for metallic Pd. The X-ray photoelectron spectroscopy (XPS, AXIS HIS, Kratos) profile revealed significant peaks of C, F, and Pd (Fig. 2c). The specific XPS spectrum of the Pd particles was also

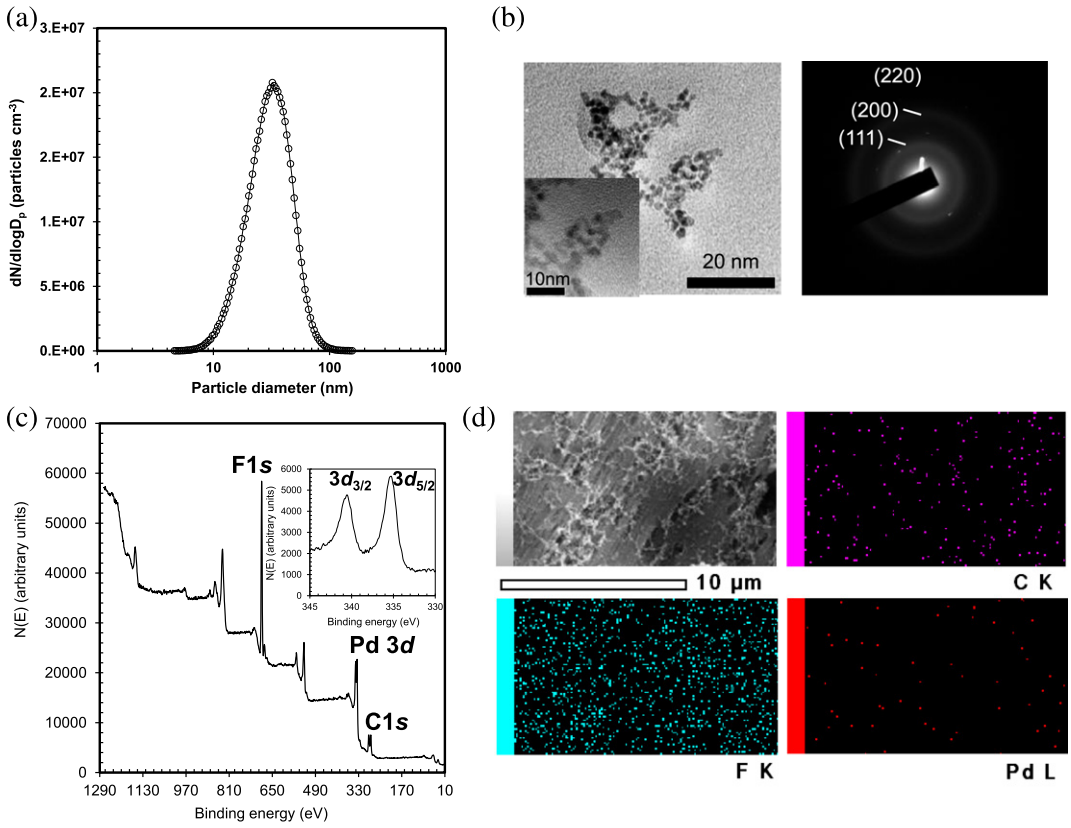

Fig. 2. Results of Pd aerosol activation. (a) Size distribution of spark generated Pd aerosol particles. (b) TEM micrographs and electron diffraction image of the Pd particles. (c) XPS spectra of the Pd particle deposited PTFE membrane and Pd particles (inset). (d) EDX maps of the Pd particle deposited membrane.

checked (inset of Fig. 2c), and the results described two Pd energy peaks assigned to the $3d_{5/2}$ and $3d_{3/2}$ energy levels located at 335.3 and 340.5 eV, respectively, which corresponded to signals from atomic Pd. Fig. 2d shows a scanning electron microscope (SEM, s-570, Hitachi) micrograph of the surface of the Pd aerosol activated membrane. As is seen from the micrograph, coverage of the Pd particles on the membrane was achieved. The following three images show the energy-dispersive X-ray (EDX) maps of the micrograph. These maps correspond to C, F, and Pd, respectively. The dots in these images indicate the existence of each element in the micrograph. It could be suggested that the activated membrane contained Pd particles whereas C and F, which might have originated from the membrane, were also detected. From the above characterizations, an activation intensity $I_a(D_p)$ of membrane is defined as follows [14,18,22]:

$$I_a(D_p) = Qt_aA_m^{-1}\int_0^{\infty}\eta(D_p)C_a(D_p)dD_p \quad (7)$$

where, Q is the flowrate of nitrogen gas, t_a the activation time, A_m the plane area of membrane, and $C_a(D_p)$ the area concentration of Pd particles. The activation intensity was selected to be approximately 6.24 cm^2 of Pd cm^{-2} of membrane (or 50.1 μg of Pd cm^{-2} of membrane).

Fig. 3a shows the SEM micrographs of the Cu deposited membranes for the presence and absence of ultrasound. For the presence of ultrasound, small particles (~40 nm) formed initially (0.5 min ELD) on the top of the Pd particles. In the process of time, Cu particles were continuously grown along with the Pd particles, and finally, for the 3 min ELD, the Cu particles became denser. It seemed that the initial deposition kinetics could be described by progressive nucleation on active sites, followed by the diffusion of Cu^{2+} ions toward the growing Cu islands and reduction to Cu atoms on the Pd particles. The deposited Cu atoms then acted as a self-catalyst for further Cu deposition, and a well-developed Cu particle layer on the membrane was then obtained. SEM micrographs for the absence of ultrasound (*i.e.* 20 and 45 °C with mechanical agitation) are also displayed in Fig. 3a, and the size of the Cu particles was noticeably larger than that in the presence of ultrasound, although the deposition trends (not shown) mostly show that the prolonged deposition increased the coverage of Cu particles on the membrane surface. The Cu deposition times to form 660 μg Cu cm^{-2} membrane were 3, 16, and 60 min for the 'ultrasound', '45 and 20 °C' cases, respectively. In comparison with the 20 and 45 °C cases, the deposition kinetics was fastest for the 'ultrasound.' This result might have originated from an enhancement of mass transport, resulting in the electrons easily transferring from HCHO to Cu^{2+} ions on the active sites [11,23]. When an ELD is performed in an ultrasound field, a number of effects enhance as a result of acoustic cavitation compared to mechanical agitation, including larger mass transport and localized heating, and thus it produces more active sites on which deposition can take place [24]. As shown in Fig. 3b, the enhanced mass transfer introduced a rapid-individual Cu growth on a number of Cu islands during ELD in the presence of ultrasound (*i.e.* ultrasound could produce finer grained Cu crystals in the initial stages of ELD which are more catalytic), while a slow-spreadable Cu growth on a few Cu islands was performed in the absence of ultrasound. Consequently, the resulting deposition rate of Cu in the presence of ultrasound was ~26.1 and ~5.4 times respectively larger than those for 25 and 45 °C with mechanical agitation (*i.e.* in the absence of ultrasound).

Fig. 3c shows the EDX spectrum for a part of the 'ultrasound:1.5 min.' The spectrum shows that the binding energy peaks at 0.93, 8.04, and 8.91 keV belong to CuL_α, CuK_α, and CuK_β, respectively. C and F might have originated from the membrane, and Au might have originated from the Au coating prior to SEM analyses.

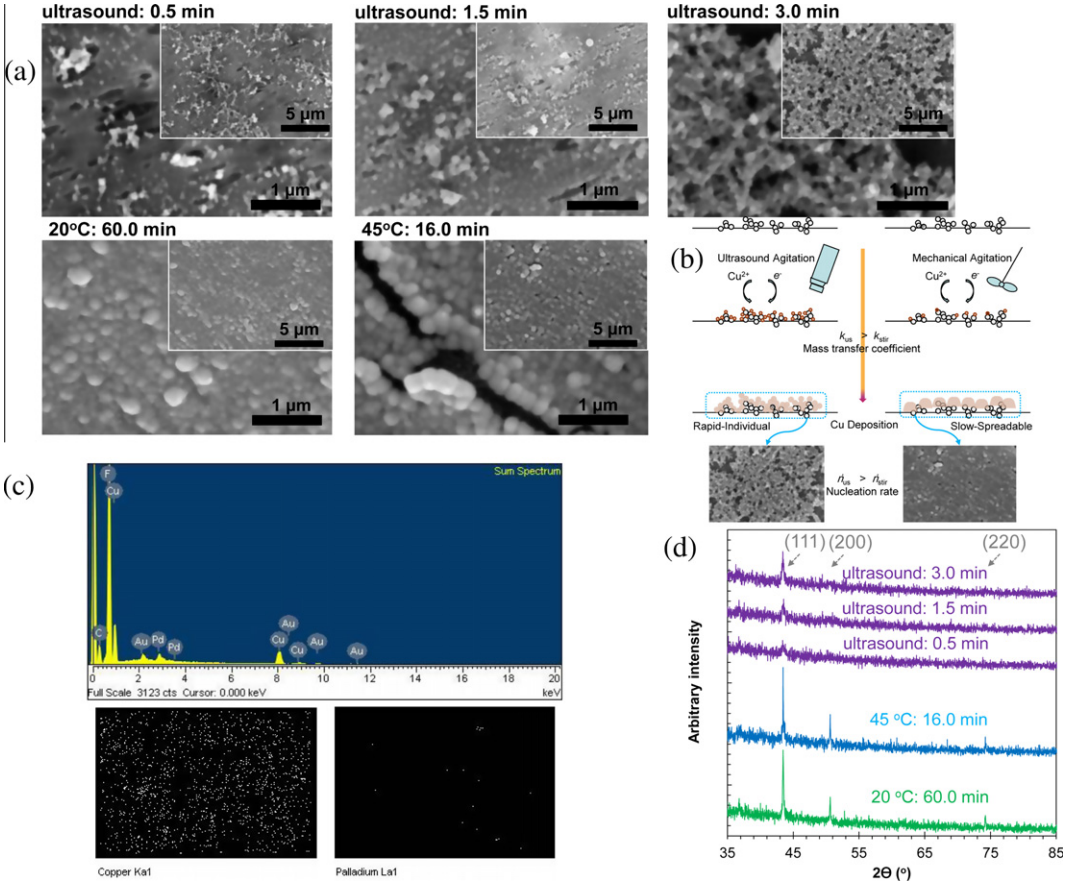

Fig. 3. Results of Cu ELD. (a) SEM micrographs of Cu ELD at ultrasound, 20, and 45 °C. (b) Scheme of Cu ELD for ultrasound and mechanical agitation. (c) EDX spectra and maps of electroless Cu deposited membrane. (d) XRD spectra of Cu ELD at ultrasound, 20, and 45 °C.

The following maps correspond to Cu and Pd, respectively, and the dots in these maps indicate the positions of elemental Cu and Pd in the first image, which shows the ELD produced metallic Cu particles. In Fig. 3d, the diffraction peak at 43.32° can be seen clearly for the all cases, but the peaks at 50.42° and 74.08° can only be seen for the absence of ultrasound (*i.e.* '20 °C: 60.0 min' and '45 °C: 16.0 min'). The relative intensity ratio of $I_{(111)}/I_{(200)}$ reached the value of 22.6 at 'ultrasound: 3.0 min', which indicated that the particles grew predominantly along the (1 1 1) lattice. Such a high intensity ratio 22.6 meant that the deposited particles were highly textured [25] and mostly consisted of <10 nm sized crystallites (*i.e.* about 10–50% of the atoms were surface atoms) [26]. The estimated sizes of Cu crystallite using Scherrer's formula were approximately 9, 27, and 32 nm for 'ultrasound: 3.0 min', '20 °C: 60.0 min', and '45 °C: 16.0 min', respectively. Correspondingly, in Fig. 3a, the size of the Cu grain in the presence of ultrasound was noticeably smaller than those in the absence of ultrasound.

Fig. 4a shows the SEM micrographs when the intensity of the ultrasound was lower ('97.4 W cm^{-2}') and a higher ('292.2 W cm^{-2}') than that in the previous ultrasound-assisted case (Fig. 3a). For the '97.4 W cm^{-2}', the decreased intensity of the ultrasound might induce a weak environment for transferring the chemical species within the bath, resulting in a larger size of the Cu particles similar to that obtained in the absence of ultrasound. For the '292.2 W cm^{-2}', an enhancement of mass transfer could induce a deposition of fine Cu particles, similar to the previous case. However, the size had no more remarkably smaller than that in the previous case. The on–off configuration (1 (or 3) s at an interval of 1 (or 3) s, *i.e.* '1 (or 3) s on–1 (or 3) s off') of the ultrasound was also tested at the same intensity as the previous ultrasound-assisted case (Fig. 4b), which further confirmed the effect on Cu deposition characteristics. Even though the ultrasound was applied with same amount of energy as in the previous case, the morphology of the Cu particles was close to the cases for the absence of ultrasound. This trend was clearer for the '3 s on–3 s off' configuration than for the '1 s on–1 s off' configuration. This may have related to P_{diss} (the power dissipated by the sonoelectrode, W), and the on–off configuration induces different $(dT/dt)_{t=0}$ values (in Eq. (8)) in P_{diss} although the same amount of energy was applied to the ELD reactions.

$$P_{diss} = \left(\frac{dT}{dt}\right)_{t=0} mC_p \tag{8}$$

where, m and C_p are the mass and heat capacity of the solvent, respectively, and $(dT/dt)_{t=0}$ is the initial slope of the temperature of the reagent versus the time it is exposed to ultrasound. Therefore, the discontinuities in the ultrasound may interrupt or delay the transferring of the chemical species on active sites, resulting in the formation of larger Cu particles.

Methanol conversion (Fig. 5a) increased with the reaction temperature and the trend was similar to previous reports [3,13]. This result was attributed to the overcoming of the limitations of internal mass transfer of the Cu particles on the membrane, owing to the rapid increase in the chemical reaction rate of methanol steam reforming with increasing reaction temperature [27]. It is found that the reactor with a Cu deposited membrane from ultrasound-assisted ELD demonstrated a better performance regarding X_{MeOH} and y_{H_2} than the results in the absence of ultrasound. From the SEM result (Fig. 3a), the reactant (methanol–water) could easily pass through the Cu deposited membrane, due to the structure of

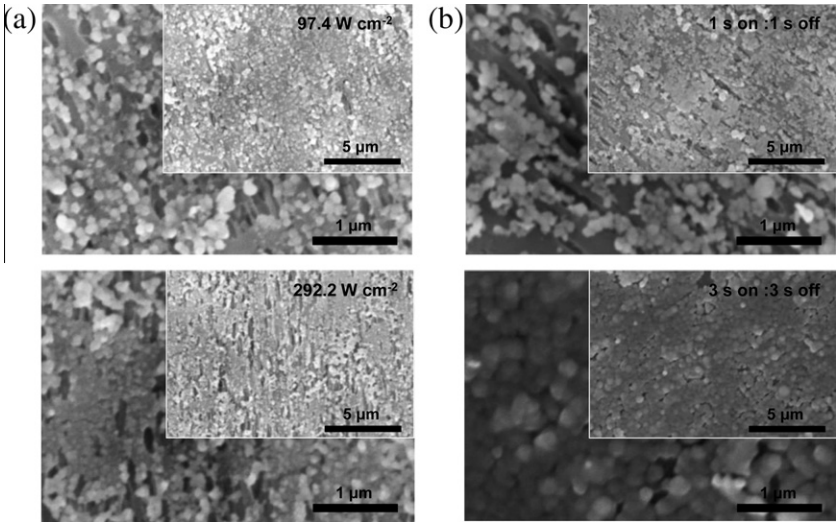

Fig. 4. SEM micrographs of ultrasound-assisted Cu ELD (a) with different ultrasound intensities and (b) configurations at the 300 μg Cu cm^{-2} membrane.

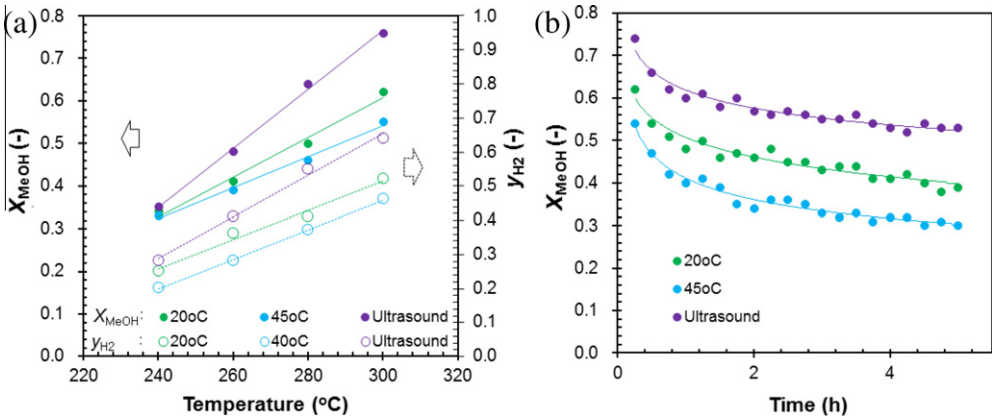

Fig. 5. Results of methanol steam reforming using electroless Cu deposited membranes (300 μg Cu cm^{-2} membrane). (a) Methanol conversion (X_{MeOH}) and corresponding hydrogen volume fraction (y_{H_2}) of the membranes from different Cu electroless bath conditions (at ultrasound, 20, and 45 °C). (b) Time dependent X_{MeOH} (at 300 °C) of the membranes from the different bath conditions.

the Cu particles (inducing a number of gas flow channels). Thus, the Cu contact area of the reactant increased, and then the reforming reaction could be effectively carried out on the surface of Cu particles. For the absence of ultrasound (in ELD, not in methanol steam reforming), the membrane was entirely covered with larger Cu particles than for the presence of ultrasound (in ELD), and this induced a decrease in the effective catalytic area which participated in the catalytic reaction. The surface area S of the Cu particles and the amount a of CO adsorbed were estimated by the following relations [12]:

$$S = \frac{6}{D_c \rho_{Cu}} \tag{9}$$

$$a = \frac{S}{NS'} \tag{10}$$

where D_c is the crystallite size of Cu (from XRD analyses), ρ_{Cu} is the specific gravity of Cu, N is Avogadro's number, and S' is the cross-sectional area of a CO molecule (0.13 nm). The estimated S (and a) values for the 'ultrasound', '20 and 45 °C' cases were 74.4 (9.5), 24.8 (3.2), and 20.9 $m^2\ g^{-1}$ (2.7×10^{-13} g mol^{-1}), respectively. The drops in conversion or more precisely the deactivation is displayed in Fig. 5b. A rapid deactivation started from the initial stage up to ~0.8 h, and then a mild rate subsequently followed up ~3.5 h. This might be due to sintering, which resulted in the loss of Cu surface area as well as in a decrease in the number of active sites [3]. According to the previous reports [28,29], the sintering of Cu metal might occur at <180 °C in the gas stream containing H_2 molecules. In addition, the formation of a carbon deposit on the Cu particles probably caused the deactivation. The carbon deposit C may be mainly formed by the Boudart reaction [12]:

$$2CO \rightarrow C + CO_2 \tag{11}$$

A further study focus on selectivity and deactivation together with the elucidation of structural features of Cu particles and their relation to the catalytic performance and mechanistic details of the catalytic reaction is now in preparation to be published elsewhere.

4. Conclusions

The application of ultrasound introduced a faster deposition (220 μg min^{-1} in deposition rate) and finer Cu particles (9 nm in crystallite size) than those (0.4 and 1.4 μg min^{-1}; 27 and 32 nm) in the absence of ultrasound (*i.e.* respectively '20 and 45 °C' with mechanical agitation). A better performance of methanol steam reforming (0.59 in mean conversion during 5 h operation; 1.3

and 1.6 times respectively higher than those from 20 to 45 °C cases) was materialized for the ultrasound application. This method is not complex, expensive, or hazardous, and also could be extended to deposit metallic Cu particles on other substrates. This may be useful for various scientific and/or engineering applications for catalyst, catalytic electrodes, *etc.*

Acknowledgment

This research was supported by the Academic Research Fund of Hoseo University in 2011 (2011-0255).

References

[1] J.-W. Kim, J.-E. Lee, J.-H. Ryu, J.-S. Lee, S.-J. Kim, S.-H. Han, I.-S. Chang, H.-H. Kang, K.-D. Suh, J. Polym. Sci., Part A: Polym. Chem. 42 (2004) 2551–2557.
[2] Y. Huang, R. Dittmeyer, J. Membr. Sci. 302 (2007) 160–170.
[3] F.-W. Chang, W.-Y. Kuo, K.-C. Lee, Appl. Catal., A 246 (2003) 253–264.
[4] D. Wu, T. Zhang, W.-C. Wang, L. Zhang, R. Jin, Polym. Adv. Technol. 19 (2008) 335–341.
[5] V. Meille, Appl. Catal., A 315 (2006) 1–17.
[6] T. Bhuvana, G.V.P. Kumar, G.U. Kulkarni, C. Narayana, J. Phys. Chem. C 111 (2007) 6700–6705.
[7] F. Touyeras, J.-Y. Hihn, M.-L. Doche, X. Roizard, Ultrason. Sonochem. 8 (2001) 285–290.
[8] F. Touyeras, J.Y. Hihn, X. Bourgoin, B. Jacques, L. Hallez, V. Branger, Ultrason. Sonochem. 12 (2005) 13–19.
[9] S. Mononobe, Jpn. J. Appl. Phys. 47 (2008) 4317–4318.
[10] Y. Lu, Appl. Surf. Sci. 256 (2010) 3554–3558.
[11] J.H. Byeon, Y.-W. Kim, Ultrason. Sonochem. 19 (2012) 209–215.
[12] Y. Liu, T. Hayakawa, K. Suzuki, S. Hamakawa, T. Tsunoda, T. Ishii, M. Kumagai, Appl. Catal., A 223 (2002) 137–145.
[13] W. Zhou, Y. Tang, M. Pan, X. Wei, H. Chen, J. Xiang, Int. J. Hydrogen Energy 34 (2009) 9745–9753.
[14] J.H. Byeon, J. Hwang, ACS Appl. Mater. Interfaces 1 (2009) 261–265.
[15] K. Ostrikov, A.B. Murphy, J. Phys. D: Appl. Phys. 40 (2007) 2223–2241.
[16] Y.-L. Liu, C.-H. Yu, J.-Y. Lai, J. Membr. Sci. 315 (2008) 106–115.
[17] J.C.S. Wu, T.Y. Chang, Catal. Today 44 (1998) 111–118.
[18] J.H. Byeon, Y.-W. Kim, ACS Appl. Mater. Interfaces 3 (2011) 2912–2918.
[19] G.-G. Park, D.J. Seo, S.-H. Park, Y.-G. Yoon, C.-S. Kim, W.-L. Yoon, Chem. Eng. J. 101 (2004) 87–92.
[20] D.J. Seo, W.-L. Yoon, Y.-G. Yoon, S.-H. Park, G.-G. Park, C.-S. Kim, Electrochim. Acta 50 (2004) 719–723.
[21] H. Yu, H. Chen, M. Pan, Y. Tang, K. Zeng, F. Peng, H. Wang, Appl. Catal., A 327 (2007) 106–113.
[22] J.H. Byeon, B.J. Ko, J. Hwang, J. Phys. Chem. C 112 (2008) 3627–3632.
[23] J. Jiang, H. Lu, L. Zhang, N. Xu, Surf. Coat. Technol. 201 (2007) 7174–7179.
[24] A.J. Cobley, T.J. Mason, V. Saez, Trans. Inst. Met. Finish. 89 (2011) 303–309.
[25] S.-K. Koh, W.-K. Choi, K.-H. Kim, H.-J. Jung, Thin Solid Films 287 (1996) 266–270.
[26] A.K. Chawla, R. Chandra, J. Nanopart. Res. 11 (2009) 297–302.
[27] H. Chen, H. Yu, Y. Tang, M. Pan, F. Peng, H. Wang, J. Yang, Appl. Catal., A 337 (2008) 155–162.
[28] A.J. Marchi, J.L.G. Fierro, J. Santamaría, A. Monzón, Appl. Catal., A 142 (1996) 375–386.
[29] Y.J. Tu, Y.W. Chen, Ind. Eng. Chem. Res. 37 (1998) 2618–2622.